Cardiovascular Pharmacology

Cellular electrophysiological effects of changrolin in isolated rat cardiac myocytes

Wei-hai Chen [a,b], Ding Yang [a,b], Wen-yi Wang [a], Jie Zhang [a], Yi-ping Wang [a,*]

[a] State Key Laboratory of Drug Research, Shanghai Institute of Materia Medica, Shanghai Institutes for Biological Sciences, Chinese Academy of Sciences, Shanghai 201203, China
[b] Graduate School of the Chinese Academy of Sciences, China

ARTICLE INFO

ABSTRACT

Changrolin (2, 6-bis[pyrrolidin-1-ylmethyl]-4-[quinazolin-4-ylamino] phenol) is an anti-arrhythmic drug derived from β-dichroine, an active component of the Chinese medicinal herb, *Dichroa febrifuga* Lour. To elucidate the mechanism underlying the anti-arrhythmic effect of changrolin, we used the whole-cell patch-clamp technique to characterize the electrophysiological actions of changrolin in isolated rat cardiomyocytes. In this study, changrolin inhibited delayed rectified K^+ currents (I_K) in a concentration-dependent manner with inhibiting the current by $11.9\% \pm 4.7\%$, $27.8\% \pm 3.4\%$, $31.5\% \pm 3.6\%$ and $40.8\% \pm 3.7\%$ at 10, 30, 100 and 300 μM, respectively ($n = 7–8$). Changrolin was less effective against transient outward K^+ currents (I_{to}), and only showed significantly inhibitory effect at the highest concentration (300 μM). Changrolin also induced a concentration-dependent inhibition of sodium currents (I_{Na}) with an IC_{50} of 10.19 μM (Hill coefficient = -1.727, $n = 6–7$). In addition, changrolin exerted a holding potential-dependent block on Na^+ channels, produced a hyperpolarizing shift in the steady-state inactivation curve, as well as exhibited a marked frequency-dependent component to the blockade of Na^+ channels. Finally, calcium currents (I_{Ca}) was decreased by changrolin in a concentration-dependent manner with an estimated IC_{50} of 74.73 μM (Hill coefficient = -0.9082, $n = 6$). In conclusion, changrolin blocks Na^+ and Ca^{2+} channels, and also blocks K^+ channels (I_{to} and I_K) to some extent. Notably, changrolin preferentially blocks the inactivated state of Na^+ channels. These effects lead to a modification of electromechanical function and likely contribute to the termination of arrhythmia.

© 2010 Elsevier B.V. All rights reserved

1. Introduction

Changrolin (2, 6-bis[pyrrolidin-1-ylmethyl]-4-[quinazolin-4-ylamino] phenol) (Fig. 1), derived from the Chinese medicinal herb, *Dichroa febrifuga* Lour, is widely used as an anti-arrhythmia drug in China. In clinical studies, changrolin was reported to be highly effective in the treatment of premature beats caused by coronary heart disease and myocarditis sequelae, and moderately effective in the treatment of atrial premature beat caused by acute myocarditis, with no obvious cardiovascular side effects (Shen et al., 1983). Other clinical trials have also shown significant therapeutic effects of changrolin on ventricular premature beats (Chen et al., 1985; Xu et al., 1987) and paroxysmal supraventricular tachycardia (Xu et al., 1987). These observations are supported by studies using animal models, which have shown that changrolin is an effective anti-arrhythmia drug(Gu et al., 1984). Furthermore, *in vitro* studies on the anti-arrhythmia mechanisms of changrolin have shown that changrolin does not only cause profound reductions in action potential amplitude (APA), action potential duration (APD) and maximal rate of phase-0 depolarization (V_{max}), but also prolong the effective refractory period (ERP) in guinea pig and rat ventricular preparations (Li, 1982; Liu et al., 1989; Pan et al., 1990).

However, the references about mechanisms underlying the efficacy of changrolin on arrhythmia focus on alteration of action potentials and the references about the direct effect of changrolin on Na^+, K^+, Ca^{2+} channels with voltage-clamp technique are limited. Therefore, the molecular basis for the anti-arrhythmic effect of changrolin is not well understood. Although some experiments have been conducted with the aim of characterizing the electrophysiological actions of changrolin on the different channels(Lu, 1999; Lu et al., 1995), the results could not entirely explain the effects of changrolin, especially on the reduction of V_{max}. As we known, reduction of maximal rate of phase-0 depolarization (V_{max}) is associated with inhibition of Na^+ channels, but the effect of changrolin on Na^+ channels is obscure and there is no available reference about the details of changrolin on Na^+ channels.

In addition, there has been a renewed focus on the safer drugs because of the side effects of anti-arrhythmia drugs and some of this attention has emphasized changrolin and its derivatives, which have been the subject of a number of studies (Li et al., 2003; Velazquez et al., 2008). The incomplete understanding of changrolin's activities and the importance of developing safer anti-arrhythmic drugs

---

Fig. 1. Chemical structure of changrolin (2,6-bis[pyrrolidin-1-ylmethyl]-4-[quinazolin-4-ylamino] phenol).

prompted us to more accurately and fully elucidate the electrophysiological actions of changrolin.

In this study, we used the whole-cell patch-clamp technique to characterize the electrophysiological actions of changrolin in isolated rat cardiomyocytes.

2. Materials and methods

2.1. Cell isolation

The animal experiments were conformed to the institutional guidelines on the care and use of experimental animals approved by the animal care and use committee of Shanghai Institute of Materia Medica, Chinese Academy of Sciences. Rat ventricle myocytes were enzymatically isolated from male Sprague-Dawley rats (180–250 g), as described previously (Alvarez et al., 2004). Briefly, rats were anaesthetized with pentobarbital sodium (50 mg/kg, i.p.) and their hearts were quickly removed, washed in the ice-cold, Ca^{2+}-free Tyrode solution (in mM: 140 NaCl, 5.4 KCl, 10 HEPES, 1 $MgCl_2$, 10 glucose; pH at 7.4) and then suspended and retrogradely perfused with Ca^{2+}-free Tyrode solution for 5 min on a heated (37 °C) Langendorff apparatus, followed by 18–22 min perfusion with the similar Ca^{2+}-free Tyrode solution with the addition of collagenase I (0.2 mg/ml, Sigma-Aldrich Inc., USA) and the bovine serum albumin (1 mg/ml, Amresco Inc. USA). All solutions were bubbled with 100% O_2. At the end of the perfusion period, the hearts were removed and transferred to a petri dish containing modified Kraftbrühe (KB) solution composed of (in mM) 80 KOH, 40 KCl, 25 KH_2PO_4, 3 $MgSO_4$, 20 taurine, 5 glutamic acid, 0.1 EGTA, 10 HEPES and 10 glucose; pH at 7.4. The ventricles of the digested heart were then cut into small pieces and mechanically agitated to free the myocytes. The cells were stored at room temperature (22 °C–26 °C) until used, normally within 6 h. Only rod-shape quiescent myocytes with clear cross-striations were used in this study.

2.2. Whole-cell patch-clamp recording

The electrophysiological experiments were carried out on a Nikon Diaphot 300 inverted microscope (Nikon, Tokyo, Japan) mounted on a vibration-isolation table. An Axopatch 200A voltage-clamp amplifier (Axon Instruments Inc., CA, USA) was used, and experiments were conducted under computer control (pClamp software 9.0, Axon Instruments, USA). An aliquot of cells was transferred to the experimental chamber, which was mounted on the stage of an inverted microscope and continuously perfused with the experimental solutions (see Solutions and chemicals) in a recording chamber (~1 ml volume) at room temperature (22 °C–26 °C). The whole-cell patch-clamp technique was used for all experiments described in this study. Electrodes with a resistance of 1–2 MΩ were used, and the tip of the electrode was filled with pipette solution (see Solutions and chemicals). The pipette solution contained 1 mM $CaCl_2$ to ensure that accidental rupture of the membrane resulted in cell death. The liquid junction potential was 5.0–6.5 mV for Na^+ current recording, 4.5–6.0 mV for K^+ current recording, and 3.0–4.0 mV for Ca^{2+} current recording. And all liquid junction potentials were corrected. After electrical access was obtained and the capacity transients became constant, series resistance was compensated and measurements were made. After forming the whole-cell recording configuration, the capacitance of the membrane was measured by applying a small depolarizing step of 5 mV from holding potentials (−80 mV). Voltage and current signals were filtered at 1 kHz (low pass) and digitized at 2 kHz.

2.3. Solutions and chemicals

The solutions used for cell isolation were described above. The ionic composition of the external solution for recording K^+ currents (I_{to}, I_K) contained (in mM) 145 NaCl, 1 $MgCl_2$, 2 KCl, 10 glucose, 10 HEPES, 1.0 $CaCl_2$, 0.05 tetrodotoxin (TTX) and 0.1 $CdCl_2$; pH was adjusted to 7.4 with NaOH. The ionic composition of the internal solution of the patching pipette contained (in mM) 140 KCl, 0.5 $MgCl_2$, 10 HEPES, 5 K_2ATP and 10 EGTA; pH was adjusted to 7.4 with KOH.

For studying Na^+ currents (I_{Na}) in ventricular myocytes, cells were superfused with an external solution that consisted of (in mM) 100 choline chloride, 20 NaCl, 5.4 KCl, 0.33 Na_2HPO_4, 10 glucose, 0.1 $CdCl_2$, 1 $CaCl_2$ and 10 HEPES; pH was adjusted to 7.4 with NaOH. The composition of the internal solution (in mM) contained 120 CsCl, 5 $MgCl_2$, 11 EGTA, 10 HEPES, 5 Na_2ATP and 1 $CaCl_2$; pH was adjusted to 7.4 with CsOH.

For recording Ca^{2+} currents (I_{Ca}), the bath solution contained (in mM) 1.8 $CaCl_2$, 5.4 KCl, 138 NaCl, 0.5 $MgCl_2$, 20 CsCl, 0.05 TTX, 10 glucose and 10 HEPES; pH was adjusted to 7.4 with NaOH. The pipette solution contained (in mM) 125 CsCl, 10 HEPES, 10 EGTA, 20 TEA-Cl and 5 MgATP; pH was adjusted to 7.4 with CsOH.

The chemicals used to prepare external and internal solutions were purchased from Sigma-Aldrich Chemical Company. Changrolin was kindly provided by the department of medicinal chemistry of Shanghai Institute of Materia Medica (Shanghai, China). Changrolin was diluted in bath solution to the desired concentration (1–300 μM) from a stock solution (100 mM in 0.4 mM HCl, stored at −20 °C) before use.

2.4. Statistical analysis

For patch-clamp experiments, data are expressed as means ± S.E.M., where n represents the cell number of experiments performed. Statistical significance was evaluated using unpaired or paired Student's t-tests and ANOVAs for multiple comparisons. A P-value < 0.05 was considered statistically significant. Concentration-response curves were fit to an equation of the form:

$$E = E_{max} \big/ \left[1 + \left([C]/IC_{50} \right)^{nH} \right] \tag{1}$$

where E is the effect at concentration [C], E_{max} is the maximal effect, and IC_{50} is the concentration for half-maximal block and nH is the Hill coefficient.

The steady-state activation curve was analyzed by determining the conductance from the equation:

$$G_m = I / (E_m - E_{rev}) \tag{2}$$

where I is the peak current, E_m is the test voltage, and E_{rev} is the estimated reversal potential, and plotting against the corresponding voltage. Plots were fitted with the Boltzmann equation:

$$G / G_{max} = 1 / 1 + \exp \left[\left(V_{1/2} - V_m \right) / k \right] \tag{3}$$

where G is the conductance following the test potential V_m, G_{max} is the maximal conductance, $V_{1/2}$ and k represent the voltage of activation midpoint and slope factor, respectively.

The steady-state inactivation curve was determined by fitting the values of the normalized current to Boltzmann equation of the following form:

$$I / I_{max} = 1 / 1 + \exp\left[\left(V_m - V_{1/2}\right) / k\right] \tag{4}$$

where I is the current amplitude following the test potential V_m, I_{max} is the maximal current, $V_{1/2}$ is the half-maximal inactivation potential and k is the slope factor of the inactivation curve.

3. Results

3.1. Effect of changrolin on delayed rectifier K^+ currents (I_K) and transient outward K^+ currents (I_{to})

Because of the distinctly different kinetics of I_{to} and I_K in the rat ventricle, each current component can be resolved from the net current, recorded in the absence of K^+ channel blockers, by including Cd^+ to block L-type Ca^{2+} channels, and TTX to block Na^+ channels. The effects of changrolin on I_{to} and I_K were further investigated by analyzing their concentration dependence. I_{to} and I_K were elicited by the depolarizations (1000 ms) to +60 mV from a holding potential of −80 mV. The I_{to} magnitude was calculated as the difference between the fast peak of the outward current and the steady-state current at the end of the pulse. I_K magnitude was calculated as the difference between the holding current and the steady-state current at the end of the voltage-clamp pulse.(Fauconnier et al., 2005) The current–voltage relationship was obtained using a series of 1000-ms test pulses between −40 and +60 mV in 10-mV steps from a holding potential of −80 mV at 0.1 Hz. Fig. 2A shows superimposed

membrane currents recorded during voltage-clamp pulses to several test potentials from a holding potential of −80 mV under control conditions, during exposure to changrolin, after washout and exposure to the I_{to} blocker, 4-aminopyridine (4-AP). Fig. 2B shows that changrolin decreased I_K in a concentration-dependent manner with inhibiting the current by 11.9%±4.7%, 27.8%±3.4%, 31.5%±3.6% and 40.8%±3.7% at 10, 30, 100 and 300 μM, respectively ($n=7$–8 from 5 animals). Changrolin produced the less effect on I_{to}; only 300 μM changrolin significantly inhibited I_{to}, reducing the current by 31.1%±4.1% ($P<0.05$, $n=7$ from 5 animals). The inhibitory effect of changrolin on I_{to} and I_K recovered by 96.4%±4.2% and 93.8%±7.8%, respectively, upon washout. Average current–voltage relationships for the I_{to} and I_K recorded before and after addition of 300 μM changrolin ($n=6$ from 5 animals) are shown in Fig. 2C.

3.2. Effect of changrolin on sodium currents (I_{Na})

After blocking K^+ currents with internal Cs^+ and blocking Ca^{2+} currents with external Cd^+, large fast inward Na^+ currents were elicited by the depolarizations of the membrane to −30 mV for 30 ms from a holding potential of −80 mV. Preliminary experiments had shown that at least 2 min were required for the cell to display identical current tracings without a reduction in initial peak current. Original current tracings under control conditions and in the presence of changrolin are shown in Fig. 3A. At the test potential of −30 mV, 10 μM changrolin reduced I_{Na} density from the control value of −44.4±5.8 pA/pF to −26.0±5.5 pA/pF. Cell capacitance was 102.7±10.6 pF ($P<0.05$, $n=7$ from 3 animals). Fig. 3B shows the concentration-dependent inhibitory effect of changrolin on I_{Na}. Peak I_{Na} declined to 89.2%±2.1%, 83.7%±2.2%, 56.0%±5.6%, 25.5%±5.4% and 14.6%±3.8% ($n=6$–7) by exposure to 1, 3, 10, 30 and 100 μM changrolin, respectively, and the effect recovered (by 54.1%±11.5%) on washout. The calculated IC_{50} was 10.19 μM (Hill coefficient = −1.727, $n=6$–7 from 3 animals).
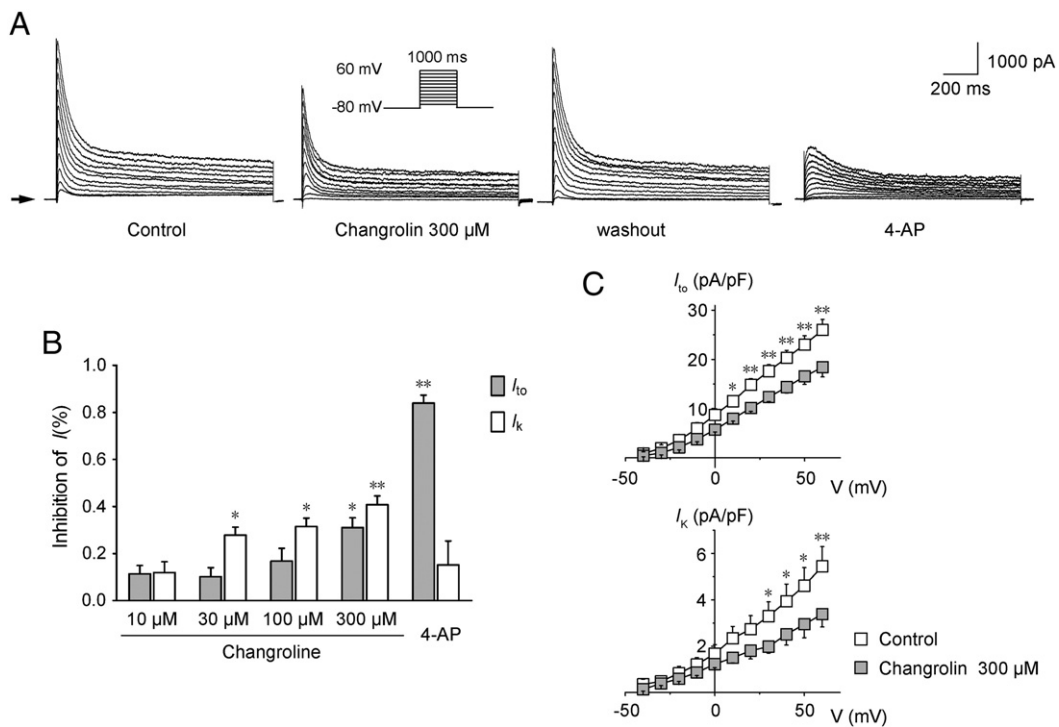
Fig. 2. Effect of changrolin on I_{to} and I_K. (A) The original superimposed recordings of I_{to} and I_K elicited by 1000-ms test pulses between −40 and +60 mV in 10-mV steps from a holding potential of −80 mV at 0.1 Hz under control conditions, after superfusion with 300 μM changrolin, washout and 5 mM 4-AP. The arrowhead in the panel indicates zero current level. (B) Changrolin inhibited I_K in a concentration-dependent manner and also inhibited I_{to} at 300 μM. (C) The current-voltage (I–V) relationship for I_{to} and I_K observed under control conditions and during exposure to 300 μM changrolin. Cell capacitance was 135.0±11.1 pF ($n=6$). Each data point represents the means ± S.E.M. *$P<0.05$, **$P<0.01$ compared with control.
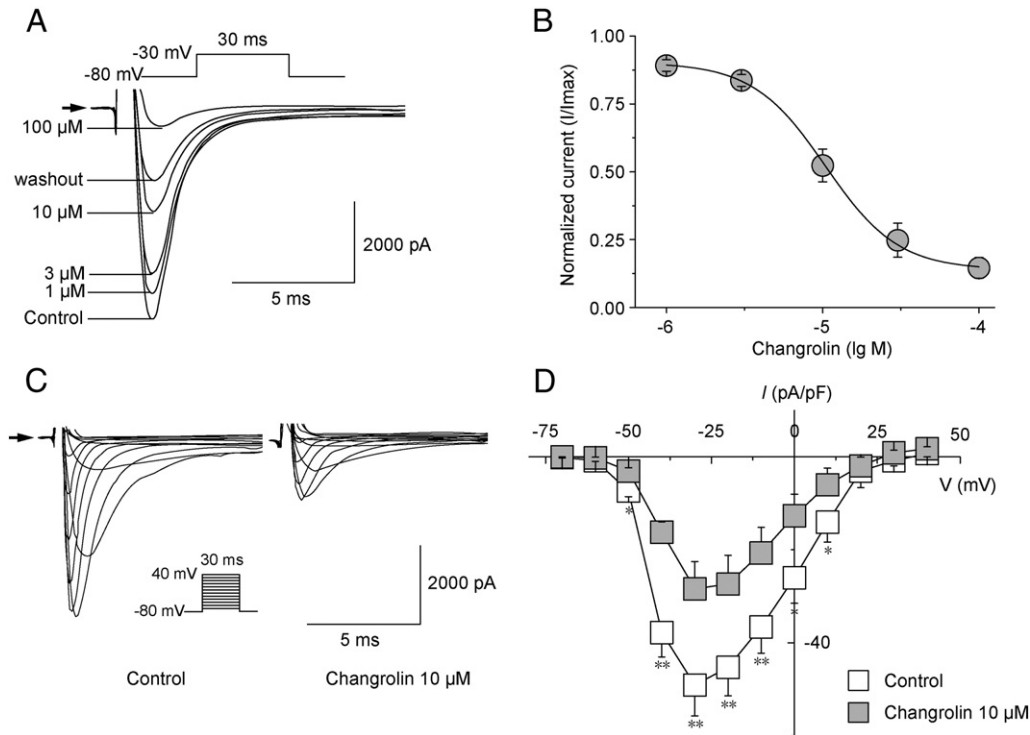
Fig. 3. Effect of changrolin on Na$^+$ channels. (A) The original recordings of I_{Na} elicited by 30-ms step depolarizations to −30 mV from a holding potential of −80 mV under control conditions, after superfusion with 1, 10, 30 and 100 μM changrolin and washout. The arrow head in each panel indicates zero current level. (B) Concentration–response curve showing the effect of changrolin on peak I_{Na}. Normalized current corresponding to the control value was plotted against drug concentration. The solid line represents a fit to the Hill equation. The calculated IC$_{50}$ was 10.19 μM (Hill coefficient was −1.727, $n = 6$–7). (C) The original superimposed recordings of I_{Na} elicited by 30-ms step depolarizations applied at 10-mV increments to different potential levels (−70 to +40 mV) from a holding potential of −80 mV at 0.2 Hz under control conditions (left) and after superfusion with 10 μM changrolin (right). (D) The current–voltage (I–V) relationship for I_{Na} observed under control conditions and during exposure to 10 μM changrolin. Cell capacitance was 102.7 ± 10.6 pF ($n = 6$). Each data point represents the means ± S.E.M. from seven cells. *$P < 0.05$, **$P < 0.01$ compared with control.

To clarify the possible mechanisms underlying the changrolin-induced reduction of I_{Na}, we studied the I_{Na} current–voltage relationship. The current–voltage relationship and activation curves were obtained using a series of test pulses from −70 mV to +40 mV with step of 10 mV from a holding potential −80 mV at 0.2 Hz. The traces in Fig. 3C show superimposed records of the currents obtained before (left) and after (right) superfusion with 10 μM changrolin. The current–voltage relationship for I_{Na} is illustrated in Fig. 3D. Under control conditions, I_{Na} was activated at the threshold potential of approximately −60 mV and attained its maximum at about −30 mV. Changrolin blocked I_{Na} without causing significant changes in the current–voltage relationship. Changrolin did not affect the voltage dependence of activation (Fig. 4A). V_h and k were −42.0 ± 0.9 mV and 4.1 ± 0.4, respectively, for controls and −39.6 ± 1.3 mV and 4.5 ± 0.2 (V_h, $P > 0.05$; k, $P > 0.05$; $n = 6$ from 3 animals) for the changrolin-treated cells.

To determine if changrolin preferentially binds to the inactivated state of the Na$^+$ channel and shifts the steady-state voltage-dependence of the inactivation curve toward more negative potentials, we characterized its effects on the voltage-dependence of steady-state inactivation. Inactivation was examined using a two-pulse protocol in which cells were first depolarized for 1 s to potentials ranging from −150 to −50 mV from a holding potential of −80 mV before measuring I_{Na} every 5 s at −30 mV (McNulty and Hanck, 2004). The effect of 10 μM changrolin on I_{Na} is shown in Fig. 4B. The smooth curves represent the best fits to the data using a Boltzmann function. Under control conditions, half-maximal current inactivation (V_h) occurred at −90.1 ± 2.3 mV, and was shifted to −102.2 ± 7.3 mV ($P < 0.01$, $n = 7$ from 4 animals) by changrolin. However, changrolin did not change the slope factor, which was 7.4 ± 0.7 under control conditions and 6.7 ± 0.3 in the

presence of 10 μM changrolin ($P > 0.05$, $n = 7$ from 4 animals). These results indicate that changrolin blocks the inactivated state of the Na$^+$ channel.

Because the results shown in Fig. 4B indicated that changrolin blocks the inactivated state of the Na$^+$ channel, it seemed likely that membrane depolarization would increase sodium channel block by changrolin. To determine if this was the case, we compared the extent of the channel blockade by changrolin (1–100 μM) on Na$^+$ channels under conditions in which all of the channels were available (−130 mV holding potential) to that under conditions in which approximately 99% of the channels were inactivated (−65 mV holding potential), using a voltage step to −30 mV to elicit I_{Na}. The results showed that changrolin is a very potent blocker when most channels are inactivated. At a holding potential of −65 mV, the IC$_{50}$ for changrolin was 6.65 μM (Hill coefficient = −1.693, $n = 6$ from 2 animals), but at a very negative holding potential (−130 mV), where virtually all channels are in the resting state, only 100 μM changrolin induced a slight reduction (13.5% ± 4.2%; $P < 0.05$, $n = 6$ from 2 animals) in the current, and an IC$_{50}$ value could not be calculated in this concentration range (1–100 μM). These results indicate that changrolin has a higher affinity for the inactivated state of the Na$^+$ channel.

3.3. Tonic and use-dependent changrolin block of Na$^+$ channels

The experiments above raised the possibility that the changrolin block is state-dependent; that is, it preferentially targets the inactivated state. To further investigate the state context of the changrolin block, we tested for tonic and use-dependent changrolin block of Na$^+$ channels. Tonic block was evaluated by holding cells at a negative potential that assured channels resided in the resting state
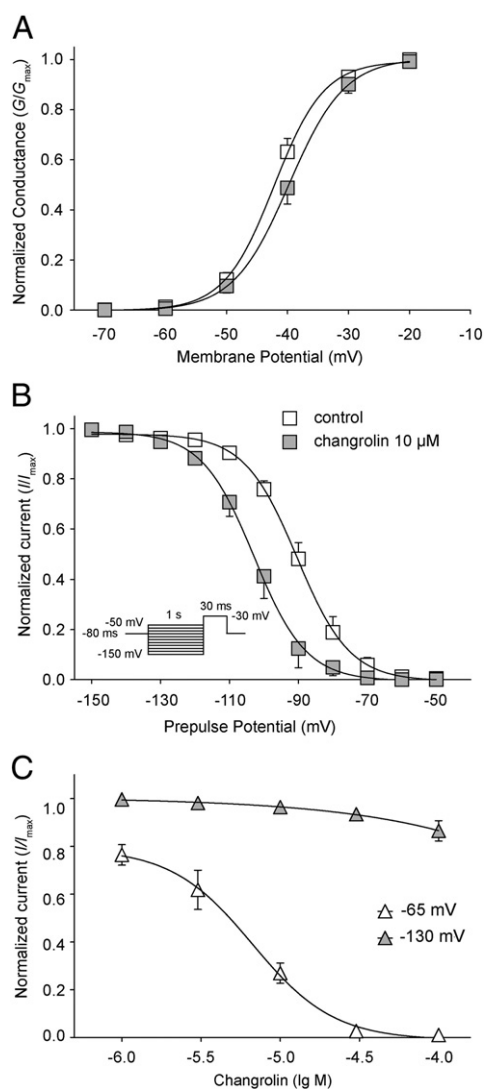
Fig. 4. Effect of changrolin on voltage-dependent steady-state activation and inactivation of Na^+ channels. The solid curves represent best fits to the Boltzmann equation (see text). Each data point corresponds to a means ± S.E.M. (A) Normalized Na^+ conductance (G_{Na}/G_{Na-max}) plotted as a function of membrane potential. Changrolin did not affect the voltage dependence for activation ($P>0.05$, $n=6$). (B) Effect of changrolin on the voltage-dependence of steady-state inactivation of Na^+ channels. The steady-state inactivation curves for the Na^+ channel were obtained by normalizing the current amplitudes (I) to the maximal value (I_{max}) and plotted as a function of the conditioning potentials in each condition. Changrolin shifted half-maximal current inactivation (V_h) 12.1 ± 1.0 mV to the negative potentials ($P<0.05$, $n=7$). (C) Concentration–response data for changrolin block of the Na^+ channel at holding potentials of −130 and −65 mV. At a holding potential of −65 mV, IC_{50} was 6.65 μM (Hill coefficient was −1.693, $n=6$), but at a holding potential of −130 mV, 100 μM changrolin slightly reduced the current by 13.5% ± 4.2% ($P<0.05$, $n=6$) and IC_{50} could not be calculated.

(−130 mV), exposing them for 5 min to 10 μM changrolin, and then initiating a train of pulses. Fig. 5A shows the superimposed records of I_{Na} obtained with repetitive depolarizing pulses at rates of 0.5 and 8 Hz. At a holding potential of −130 mV, there was no significant tonic block by 10 μM changrolin. At 0.5 Hz, the amplitude of I_{Na} evoked by the first pulse in the pulse train was 2.5 ± 0.2 nA in control conditions and 2.3 ± 0.1 nA with changrolin ($P>0.05$, $n=7$ from 2 animals), and at 8 Hz, the corresponding values were 2.4 ± 0.1 nA and 2.2 ± 0.2 nA ($P>0.05$, $n=7$ from 2 animals; Fig. 5B). The amplitude of I_{Na} induced by each pulse successively applied is plotted in Fig. 5C. In the absence of changrolin, 16 successive pulses to −30 mV for 30 ms produced no significant decrease in I_{Na}, even at a high frequency. In the presence of 10 μM Changrolin, I_{Na} amplitude became successively

smaller and then reached a steady-state level at 4 Hz and 8 Hz (Fig. 5C). The averaged final currents normalized to the first currents were 1.00 ± 0.02 at 0.5 Hz, 0.91 ± 0.02 at 4 Hz (compared with 0.5 Hz, $P<0.05$, $n=7$) and 0.81 ± 0.02 at 8 Hz (compared with 0.5 Hz, $P<0.01$, $n=7$; Fig. 5D).

3.4. Effect of changrolin on calcium currents (I_{Ca})

The holding potential was set to −40 mV to inactivate I_{Na}, and a 250-ms depolarizing pulse to 0 mV was applied (Chang et al., 2002). The reduction of I_{Ca} with time (rundown) was more prominent during the initial 5 to 10 min after rupture of the membrane patch with no significant change 20–30 min thereafter. Therefore, experiments were performed only on those cells with stable I_{Ca} (10 min after rupture). Fig. 6A shows that changrolin-induced decrease in the Ca^{2+} currents was dose-dependent. At concentrations of 1, 3, 10, 30, 100 and 300 μM, changrolin decreased I_{Ca} to 97.4% ± 0.6%, 90.2% ± 2.7%, 83.9% ± 1.8%, 66.9 ± 2.2%, 38.4% ± 3.7% and 17.0 ± 2.5%, respectively and reversed (by 55.9% ± 3.6%) on washout ($n=6$ from 3 animals). Fig. 6A (right) shows nifedipine 0.1 μM could dramatically inhibited I_{Ca}. The data were fit to the Hill equation, and the estimated IC_{50} calculated from the concentration-response curve was 74.73 μM (Hill coefficient = −0.9082, $n=6$) (Fig 6B) .Fig. 6C illustrates the superimposed traces of I_{Ca} obtained from a rat ventricular cell under control conditions (left) or changrolin (right). At the test potential of 0 mV, 30 μM changrolin reduced the I_{Ca} density from the control value of −13.3 ± 1.6 pA/pF to −9.0 ± 1.1 pA/pF. Cell capacitance was 127.1 ± 7.0 pF ($P<0.05$, $n=6$ from 3 animals). The Current–voltage relationships were obtained using a series of test pulses between −30 mV and + 60 mV with step of 10 mV from a holding potential −30 mV at 0.2 Hz. The current–voltage relationship for I_{Ca} under control conditions and after superfusion with 30 μM changrolin is illustrated in Fig. 6D. Changrolin blocked I_{Ca} without causing significant changes in the current–voltage relationship.

3.5. Effect of changrolin on voltage-dependent steady-state activation and inactivation of Ca^{2+} channels

The activation curves shown in Fig. 7A were obtained from the normalized conductance of the Ca^{2+} channel (G_{Ca}/G_{Ca-max}), calculated from the I_{Ca} amplitude data in Fig. 6C. The solid line drawn through the data points represents the best fit to the Boltzmann equation. The average values of V_h and k were −7.2 ± 1.6 mV and 5.1 ± 0.4 ($n=5$ from 3 animals), respectively, under control conditions, and −7.3 ± 2.0 mV and 5.7 ± 0.3 in the presence of 30 μM changrolin. The voltage dependence of activation was not affected (V_h, $P>0.05$; k, $P > 0.05$ $n=5$ from 3 animals). The steady-state inactivation was obtained using a conventional double-pulse protocol (Zahradnik et al., 2008). The holding potential was set to −50 mV, and the test pulses were preceded by 5-s prepulses to different inactivation voltage levels (from −50 mV to 10 mV) separated from the test pulse by a 15 ms return to −50 mV. As shown in Fig. 7B, changrolin (30 μM) did not affect the voltage dependence of inactivation. On average, V_h and k were −24.1 ± 0.9 mV and 4.5 ± 0.2 under control conditions, and −24.8 ± 0.7 mV and 4.5 ± 0.1 in the presence of 30 μM changrolin (V_h, $P>0.05$; k, $P > 0.05$; $n=9$ from 3 animals).

4. Discussion

The most significant finding arising from this study was the demonstration that changrolin blocks I_{Na}, I_{Ca}, I_K and I_{to}. These results are consistent with findings from the studies about the effect of changrolin on action potential (Li, 1982; Liu et al., 1989; Pan et al., 1990), which have also shown that changrolin reduces APA, V_{max} and APD, and prolongs ERP in guinea pig and rat ventricular preparations. Thus, the observation that changrolin is a potent blocker of Na^+
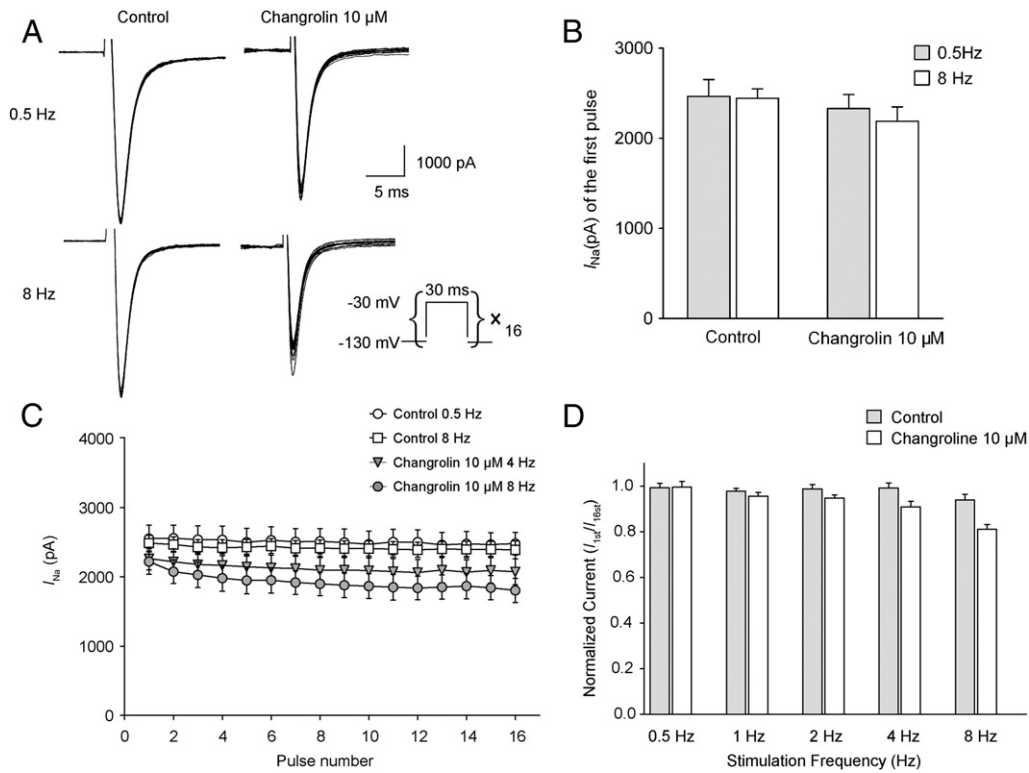
Fig. 5. Effects of changrolin on tonic and use-dependent block of Na^+ channels. (A) Superimposed recordings obtained during a train of 16 successive depolarizing pulses applied at a frequency of either 0.5 or 8 Hz before and during exposure to changrolin (10 μM). The pulse protocol used is shown in the inset of A. (B) Tonic block of changrolin on the first pulse in the pulse train at 0.5 and 8 Hz. At a holding potential of −130 mV, there was no significant tonic block at 10 μM changrolin. (C) Relationship between peak I_{Na} and number of pulses applied at different rates under control conditions and in the presence of changrolin. (D) Pooled data from five frequencies demonstrating greater block by changrolin at higher frequencies. Each data point represents the means ± S.E.M. *$P<0.05$, **$P<0.01$ compared with 0.5 Hz.
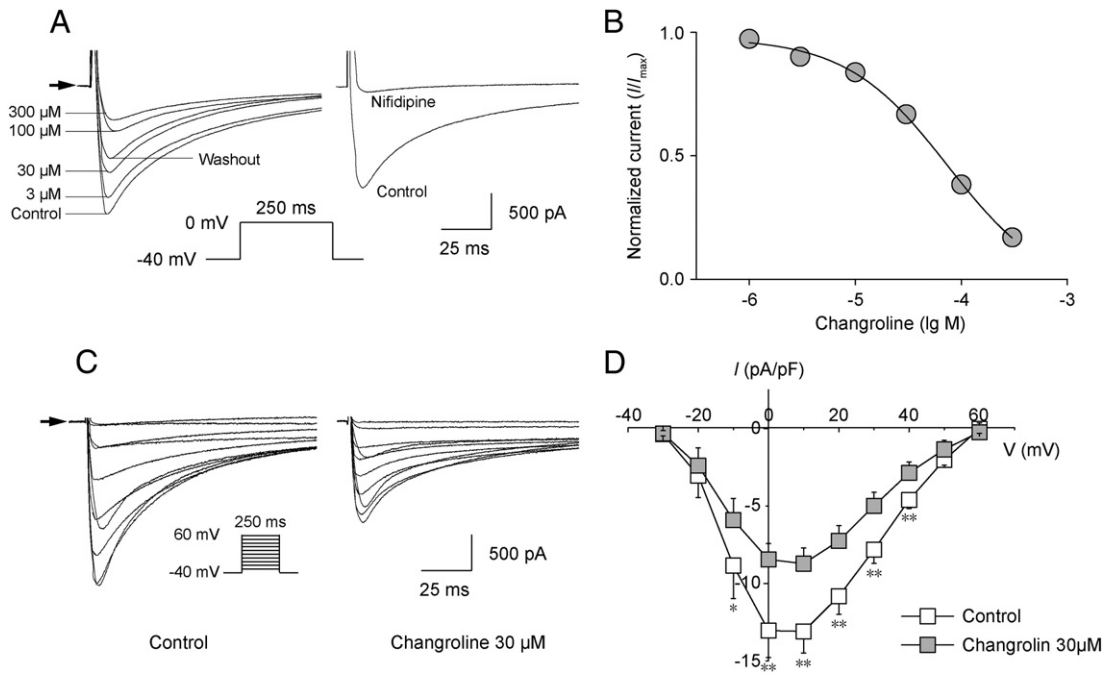
Fig. 6. Effect of changrolin on I_{Ca}. (A) The original recordings show that the concentration-dependence of inhibitory effect of changrolin on I_{Ca} (left) and inhibitory effect of 0.1 μM nifedipine on I_{Ca} (right). The arrow head in each panel indicates zero current level. (B) Concentration–response curve showing the effect of changrolin on I_{Ca}. Normalized current corresponding to the control value was plotted against drug concentration. Symbols correspond to means ± S.E.M., and the solid line represents a fit to the Hill equation. and the calculated IC_{50} was 74.73 μM (Hill coefficient was −0.9082, $n=6$). (C) The original superimposed recordings of I_{Ca} elicited by 250-ms step depolarizations applied at 10-mV increments every 5 s to different potentials between −30 and +60 mV from the holding potential of −40 mV under control conditions, and after superfusion with 30 μM changrolin or 0.1 μM nifedipine. The arrow head in the panel indicates zero current level. (D) The current-voltage (I–V) relationship for I_{Ca} observed under control conditions and during exposure to 30 μM changrolin. Cell capacitance was 127.1 ± 7.0 pF ($n=6$). Each data point represents the means ± S.E.M. from six cells. *$P<0.05$, **$P<0.01$ compared with control.
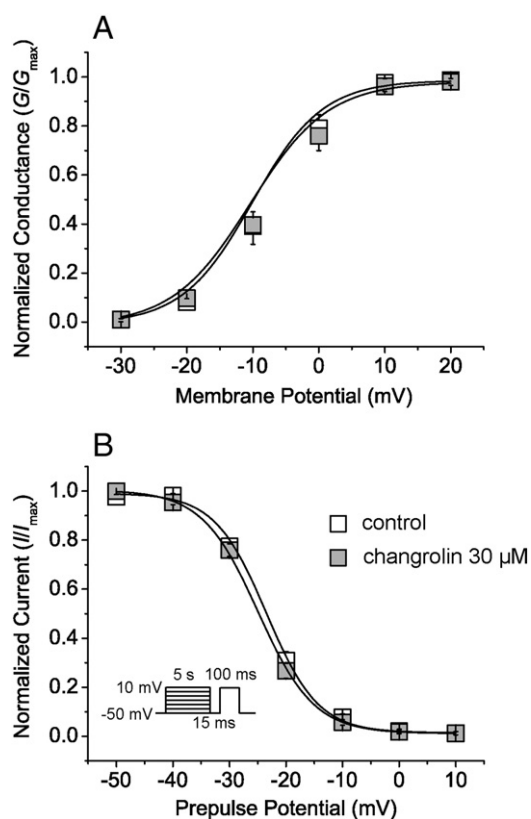
Fig. 7. Voltage dependence of steady-state activation and inactivation of the Ca^{2+} channel in the absence and presence of 30 μM changrolin. (A) The activation curves were obtained from the normalized conductance of the Ca^{2+} channel (G_{Ca}/G_{Ca-max}), calculated from the I_{Ca} amplitude data in Fig. 6C, and plotted as a function of the depolarizing potentials. The solid line drawn through the data points represents the best fit to the Boltzmann equation. Changrolin did not affect the voltage dependence for activation. ($P > 0.05$, $n = 5$). (B) Steady-state inactivation examined using a double pulse protocol. The holding potential was set to −50 mV, and test pulses to different inactivating voltage levels (−50 mV to 10 mV) were preceded by 5 s prepulses separated from the test pulse by a 15 ms return to −50 mV. The inactivation curves for I_{Ca} were obtained by plotting normalized current amplitudes (I/I_{max}) as a function of the conditioning potentials before and after 30 μM changrolin. The solid line drawn through the data points represents the best fit to the Boltzmann equation. Changrolin did not affect the steady-state inactivation ($P > 0.05$, $n = 9$).

channels (I_{Na}), Ca^{2+} channels (I_{Ca}), and delayed rectifier K^+ current (I_K), demonstrated here, may account for the observed anti-arrhythmic activity of this compound.

According to the modulated receptor hypothesis, the potency of cardiac Na^+ channel blockade by class I agents differs when the channel exist in a resting, activated or inactivated state (Hille, 1977; Hondeghem and Katzung, 1977). In this study, we have clarified the mechanisms of action of changrolin on different states of the Na^+ channel. Our results indicate that changrolin had slight effect on the resting state of the Na^+ channel (i.e., at a holding potential of −130 mV). Instead, changrolin shifted the inactivation curve toward hyperpolarizing potentials and strongly inhibited I_{Na} from a holding potential of −65 mV, indicating that changrolin preferentially blocks the inactivated state of the Na^+ channel. Previous studies have reported that changrolin had no effect on the Na^+ channel (Lu et al., 1995). However, in those experiments, the holding potential was set to −120 mV, a condition in which most Na^+ channels were in the resting state. Viewed in the context of the state-dependency block of changrolin on Na^+ channels demonstrated in the current study, these previous findings, which also contradict other reports, cannot be considered conclusive. The preferential block of the inactivated state of the Na^+ channel suggests that changrolin might reduce the excitability of heart tissue, especially under pathological conditions

associated with membrane depolarization, for example, acute myocardial ischemia (Shaw and Rudy, 1997).

We also observed a use-dependent inhibition of the Na^+ channel in the cells treated with changrolin at a holding potential of −130 mV, but saw no evidence of tonic block. These results are consistent with our finding that changrolin interacts with the inactivated state of the Na^+ channel. The phenomenon of use-dependent block is generally interpreted as a drug molecule binding to channels in an open and/or inactivated state during membrane depolarization. Since Na^+ channels spend more time in the open and inactivated state as the interpulse interval shortens, the decrease in I_{Na} at high rates of stimulation reflects an accumulation of drug-associated channels. Inhibition of cardiac I_{Na} by changrolin was enhanced at high frequencies of stimulation, an observation that is consistent with previously reported effects of changrolin on action potentials in *in vitro* studies (Liu et al., 1989). The lack of a tonic component of I_{Na} block suggests that changrolin has a low affinity for the resting state of the Na^+ channel.

Previous studies have reported that changrolin reduced APA and V_{max}, shortened APD, as well as prolonged ERP in guinea pig and rat ventricular preparations (Li, 1982; Liu et al., 1989; Pan et al., 1990). The results of the current study are consistent with these previous reports on alteration of action potential, and suggest that the observed effects of changrolin on action potential arise from inhibitory effects of changrolin on multiple channels. The blockade on Na^+ channels is universally considered to account for a reduction in V_{max}. In this study, we found that changrolin, at relatively high concentrations, inhibited I_{to} and I_K. Although APD prolongation theoretically could be resulted from inhibition of these K^+ currents, which contribute to ventricular repolarization, changrolin was previously shown to shorten the APD. This apparent disparity may be resulted from concurrent inhibition of I_{Na} and I_{Ca}, which could counterbalance the inhibition of I_{to}, especially the case for the inhibitory effect of changrolin on I_{Na}, which is more potent than the inhibition on I_{to}. Furthermore, it has been reported that block of I_{Na} and/or I_{Ca}, by reducing the risk of early after-depolarization development with excessive APD prolongation and attenuating excessive repolarization duration and temporal or spatial dispersion of APD, may contribute to reducing the pro-arrhythmic potential of multi-channel blockers (Abrahamsson et al., 1996; Amos et al., 2001).

A limitation of this study is that the experiments did not exclude the possibility that changrolin may have actions on the open state of the Na^+ channel. Although our data support preferential binding of changrolin to the inactivated state, it is hard to conclude that changrolin does not bind to open channels because use-dependency experiments could not discern a binding affinity for the open or inactivated state. A definitive assessment of possible interactions of changrolin with the open state of the Na^+ channel would require experiments using inactivation-deficient Na^+ channels. In addition, this study revealed that changrolin inhibits I_K in rat ventricular myocytes, suggesting the possibility that changrolin might block the human ether-a-go-go-related gene (hERG) channel, $K_V11.1$, in human ventricular myocytes. Suppression of hERG channels causes action potential and QT interval prolongation. This, in turn, could cause long-QT syndrome and torsade de pointes (TdP), which could degenerate into ventricular fibrillation and sudden cardiac death. Therefore, assessing the effect of changrolin on hERG is an important avenue for future research.

In conclusion, we have clarified the electrophysiological mechanisms of changrolin on arrhythmia, showing that changrolin exhibits a multi-current-blocking profile in rat ventricular preparations, inhibiting I_{Na}, I_{Ca}, I_K and I_{to}. At low concentrations, block of I_{Na} predominates and is the major mechanism for alteration of APD. At higher concentrations, ancillary block of I_{Ca}, I_K and I_{to} becomes apparent. By attenuating excessive repolarization delay and spatial and temporal dispersion of repolarization, block of I_{Ca} as well as I_{Na} may be the

mechanism that accounts for the reduced proarrhythmic potential of changrolin. Collectively, these results suggest that a combination of Na$^+$, K$^+$ and Ca^{2+} channel-blocking actions may be the ideal criterion for use in developing novel changrolin derivatives that have low toxicity and relatively high efficacy, and are reasonably tolerated.

Acknowledgments

References

Abrahamsson, C., Carlsson, L., Duker, G., 1996. Lidocaine and nisoldipine attenuate almokalant-induced dispersion of repolarization and early afterdepolarizations in vitro. J Cardiovasc Electrophysiol 7, 1074–1081.

Alvarez, J., Hamplova, J., Hohaus, A., Morano, I., Haase, H., Vassort, G., 2004. Calcium current in rat cardiomyocytes is modulated by the carboxyl-terminal ahnak domain. J Biol Chem 279, 12456–12461.

Amos, G.J., Abrahamsson, C., Duker, G., Hondeghem, L., Palmer, M., Carlsson, L., 2001. Potassium and calcium current blocking properties of the novel antiarrhythmic agent H 345/52: implications for proarrhythmic potential. Cardiovasc Res 49, 351–360.

Chang, G.J., Su, M.J., Hung, L.M., Lee, S.S., 2002. Cardiac electrophysiologic and antiarrhythmic actions of a pavine alkaloid derivative, O-methyl-neocaryachine, in rat heart. Br J Pharmacol 136, 459–471.

Chen, W.Z., Wang, C.G., Yang, X.Y., Cai, N.S., Zhu, J.R., 1985. Clinical pharmacokinetics of the anti-arrhythmic agent changrolin. Yao Xue Xue Bao 20, 505–508.

Fauconnier, J., Lacampagne, A., Rauzier, J.M., Fontanaud, P., Frapier, J.M., Sejersted, O.M., Vassort, G., Richard, S., 2005. Frequency-dependent and proarrhythmogenic effects of FK-506 in rat ventricular cells. Am J Physiol Heart Circ Physiol 288, H778–H786.

Gu, C.G., Chen, W.Z., Dong, Y.L., Ding, G.S., 1984. Anti-arrhythmic effect of changrolin combined with nicotinamide in experimental arrhythmia. Zhongguo Yao Li Xue Bao 5, 173–177.

Hille, B., 1977. Local anesthetics: hydrophilic and hydrophobic pathways for the drug-receptor reaction. J Gen Physiol 69, 497–515.

Hondeghem, L.M., Katzung, B.G., 1977. Time- and voltage-dependent interactions of antiarrhythmic drugs with cardiac sodium channels. Biochim Biophys Acta 472, 373–398.

Li, Y., Yang, Z.S., Zhang, H., Cao, B.J., Wang, F.D., Zhang, Y., Shi, Y.L., Yang, J.D., Wu, B.A., 2003. Artemisinin derivatives bearing Mannich base group: synthesis and antimalarial activity. Bioorg Med Chem 11, 4363–4368.

Li, Z.Y., 1982. Effect of anti-arrhythmic drug changrolin on fast and slow response potentials of myocardial cell of rats. Zhongguo Yao Li Xue Bao 3, 172–175.

Liu, Q.Y., Chen, W.Z., Wei, P.J., Gu, P.K., Jin, Z.J., 1989. Electrophysiological effects of changrolin on single ventricular myocytes isolated from adult guinea pig. Zhongguo Yao Li Xue Bao 10, 526–529.

Lu, L.L., 1999. Effects of changrolin on potassium currents in guinea pig and rabbit single heart cells. Zhongguo Yao Li Xue Bao 20, 1015–1018.

Lu, L.L., Habuchi, Y., Tanaka, H., Morikawa, J., 1995. Electrophysiological effects of changrolin, an anti-arrhythmic agent derived from Dichroa febrifuga, on guinea-pig and rabbit heart cells. Clin Exp Pharmacol Physiol 22, 337–341.

McNulty, M.M., Hanck, D.A., 2004. State-dependent mibefradil block of Na + channels. Mol Pharmacol 66, 1652–1661.

Pan, H., Shen, W.Q., Yu, Z.M., Xu, B., 1990. Frequency- and voltage-dependent effects of changrolin on maximal upstroke velocity of action potentials in guinea pig papillary muscles. Zhongguo Yao Li Xue Bao 11, 317–321.

Shaw, R.M., Rudy, Y., 1997. Electrophysiologic effects of acute myocardial ischemia: a theoretical study of altered cell excitability and action potential duration. Cardiovasc Res 35, 256–272.

Shen, Y.T., Xu, N.S., Gu, S.L., Wu, P.M., 1983. Effects of intravenous infusion of changrolin on cardiac function of patients with arrhythmia. Zhongguo Yao Li Xue Bao 4, 251–253.

Velazquez, A.M., Martinez, L., Abrego, V., Balboa, M.A., Torres, L.A., Camacho, B., Diaz-Barriga, S., Romero, A., Lopez-Castanares, R., Angeles, E., 2008. Synthesis and antihypertensive effects of new methylthiomorpholinphenol derivatives. Eur J Med Chem 43, 486–500.

Xu, J.M., Yin, X.L., Chen, Y.M., Qi, H.M., Li, C.F., Shen, L.Y., Chen, W.Z., Wang, C.G., 1987. Plasma drug concentration and cardiac function in arrhythmic patients during continuous drip of changrolin. Zhongguo Yao Li Xue Bao 8, 227–231.

Zahradnik, I., Minarovic, I., Zahradnikova, A., 2008. Inhibition of the cardiac L-type calcium channel current by antidepressant drugs. J Pharmacol Exp Ther 324, 977–984.